Measurement of Absolute Blood Flow Velocity and Blood Flow in the Human Retina by Dual-Beam Bidirectional Doppler Fourier-Domain Optical Coherence Tomography

René M. Werkmeister,[1] *Nikolaus Dragostinoff,*[1] *Stefan Palkovits,*[2] *Reinhard Told,*[1,2] *Agnes Boltz,*[1,2] *Rainer A. Leitgeb,*[1] *Martin Gröschl,*[3] *Gerhard Garhöfer,*[2] *and Leopold Schmetterer*[1,2]

Purpose. The present experiments were undertaken to evaluate the validity of absolute flow velocity measurements with a dual-beam bidirectional Doppler Fourier-domain optical coherence tomography (FD-OCT) system.

Methods. The flow velocities of diluted milk through a glass capillary were measured at 30 different preset velocities in the range of 0.9 to 39.3 mm/s by bidirectional Doppler FD-OCT. The flow through the capillary was controlled by two infusion pumps working in different flow ranges and based on different technical principles. In vivo the validity of the method for measuring blood flow in retinal vessels was tested at bifurcations. The continuity equation was verified at 10 retinal venous bifurcations of 10 young healthy subjects (mean age, 29 ± 3 years) by velocity measurements, using dual-beam bidirectional Doppler FD-OCT, and measurements of retinal diameters, using the Dynamic Vessel Analyzer.

Results. Flow velocities as measured with bidirectional Doppler FD-OCT in the glass capillary were in good agreement with the preset velocities ($r = 0.994$, $P < 0.001$ each). No significant difference was found between flow in the trunk vessels before the bifurcation (11.3 ± 5.2 μL/min) and the sum of flows in the daughter vessels (10.7 ± 4.8 μL/min). A significant association was found between retinal vessel diameters and both retinal blood velocities ($r = 0.72$, $P < 0.001$) and retinal blood flow ($r = 0.95$, $P < 0.0001$).

Conclusions. Dual-beam bidirectional Doppler FD-OCT delivered accurate retinal blood velocity values and, thus, offers high potential for examination of retinal blood flow in ocular disease. (*Invest Ophthalmol Vis Sci.* 2012;53:6062–6071) DOI: 10.1167/iovs.12-9514

From the [1]Center for Medical Physics and Biomedical Engineering and the [2]Department of Clinical Pharmacology, Medical University of Vienna, Vienna, Austria; and the [3]Institute of Applied Physics, Vienna University of Technology, Vienna, Austria.

Supported by Fonds zur Förderung der Wissenschaftlichen Forschung (FWF), Project No. APP21570FW, Die Österreichische Forschungsförderungsgesellschaft (FFG) Project FA 607A0502, Christian Doppler Laboratory for Laser Development and their Application in Medicine.

Submitted for publication January 16, 2012; revised June 9 and July 5, 2012; accepted August 4, 2012.

Disclosure: **R.M. Werkmeister**, None; **N. Dragostinoff**, None; **S. Palkovits**, None; **R. Told**, None; **A. Boltz**, None; **R.A. Leitgeb**, None; **M. Gröschl**, None; **G. Garhöfer**, None; **L. Schmetterer**, None

Corresponding author: Leopold Schmetterer, Center for Medical Physics and Biomedical Engineering, Währinger Gürtel 18-20, A-1090 Vienna, Austria; leopold.schmetterer@meduniwien.ac.at.

Several ocular diseases, including glaucoma, diabetic retinopathy, and age-related macular degeneration, have been linked to retinal and choroidal perfusion abnormalities.[1,2] The development of a valid and reproducible technique for the measurement of retinal blood flow that is easily applicable in humans is therefore of considerable interest. A variety of techniques have been developed, which all suffer from implicit limitations. Color Doppler imaging, an ultrasound technique, allows for measurement of blood flow in large retrobulbar vessels.[3,4] Since no absolute information on the vessel diameter can be obtained, the calculation of total blood flow is, however, impossible.[3] Combined with an assessment of retinal vessel diameters, laser Doppler velocimetry (LDV) enables measurement of absolute blood flow in individual retinal vessels.[5–8] By measuring all vessels entering the optic nerve head, total retinal flow can be calculated, which, however, requires a relatively long acquisition time.[9] Today, clinical praxis relies on fluorescein and indocyanine green angiographies as the methods of choice for examination of retinal and choroidal circulation. However, attempts to extract quantitative information on blood flow[10] have not found their way into clinical practice, mostly because of their methodologic limitations to assess absolute blood flow. In addition, the technique requires injection of dyes to contrast ocular vessels, which can have some adverse effects.[11,12]

Optical coherence tomography (OCT)[13,14] is a noninvasive high-resolution imaging technique that offers the possibility of performing in vivo optical "biopsy" of tissue structures, for example, human retina[15,16] and choroid,[17,18] and thus, allows for diagnosis and treatment monitoring of ocular diseases.[19–21]

OCT can be extended to Doppler OCT by detecting phase shifts of the back-scattered light, which are caused by moving particles in the probed volume, that is, red blood cells (RBCs).[22,23] Several approaches, using two probe beams, have been introduced to overcome the problem of the a priori unknown Doppler angle for measurement of absolute velocity values[24,25] or to gain insight into blood flow in microvessels.[26] We have recently developed a dual-beam bidirectional Doppler FD-OCT device that measures absolute blood flow velocities in human retinal vessels.[27] In this article we report on several in vitro and in vivo experiments investigating the validity of data obtained with this technique.

Methods

Dual-Beam Bidirectional Doppler FD-OCT

Dual-beam bidirectional Doppler FD-OCT measurements were performed with a system based on a setup published previously.[27] Briefly, the sample, that is, the velocity vector $\vec{v}$ under study, is illuminated by

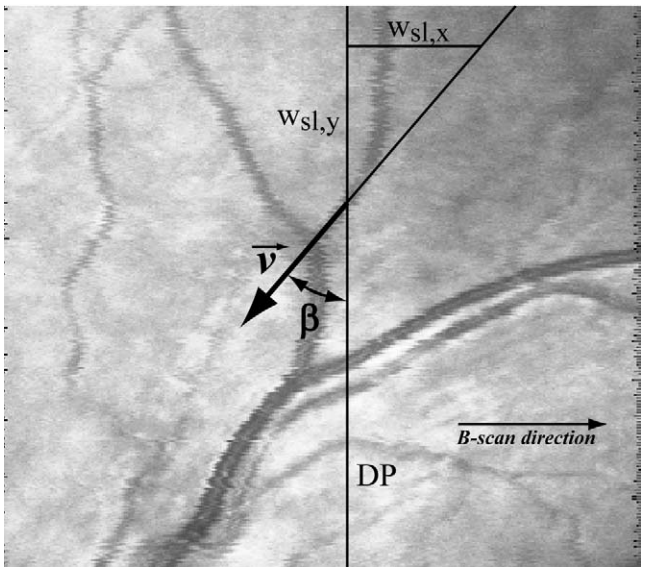

Figure 1. SLO image of a venous junction. Angle β is determined from the slope of the tangent to the vessel at the measured location. $w_{sl,x}$, $w_{sl,y}$; image width in x and y direction. DP, detection plane.

two probe beams represented by their wave number vectors, $\vec{K}_1$ and $\vec{K}_2$. Both beams are separated by their polarization properties. The light detected from each probing channel is guided into two identical spectrometers, where the spectral modulations are detected as a function of frequency. Expecting the incident and scattered wave vectors to be collinear, the phase shifts $\Phi'_{1,2}$, caused by the scattering of the impinging wave on the RBC, are given by $\Phi'_i = 2\vec{K}_i\vec{v}_i\tau$ $(i = 1, 2)$, where $\vec{v}_i$ is the velocity vector of the moving RBC pointing in the direction of the corresponding probe beam and τ is the time span between two subsequent recordings, equaling the exposure time of the camera. Φ' is directly obtained from the phase shift between adjacent A-scans as $\Phi'(z) = \arg[I^*_{n+1}(z) \times I_n(z)]$, where z is the axial position, $I_n(z)$ is the complex signal calculated by inverse fast Fourier transform (FFT) of the nth scan, and I^* is the complex conjugate.

It can be shown that the absolute value of the flow velocity is given as[27]

$$V_{abs} = \Delta\Phi \frac{\lambda}{4\pi \times n \times \tau \times \Delta\alpha \times \cos\beta}, \quad (1)$$

where $\Delta\Phi$ is the phase difference between the two probing channels, that is, $\Delta\Phi = \Phi_1 - \Phi_2$. Φ_i are postprocessed phase shifts, λ is the central wavelength of the light source, τ is the time span between two subsequent recordings of the charge-coupled device (CCD) camera, β is the angle of the velocity vector with respect to the detection plane spanned by $\vec{K}_1$ and $\vec{K}_2$, and n denotes the group refractive index of blood, which was—as an average of the values for 632.8 nm and 1080 nm[28]—estimated to be 1.37. With a parallel displacement of the two probe beams of 2 mm, the separation angle $\Delta\alpha$ at the ocular fundus for a standard eye length of 24.2 mm[29,30] is 4.7°. Obviously, equation (1) is an approximation because the sine of the angle is replaced by the angle itself. As long as the angle of incidence is close to 90°, the error is small. When the Doppler angle is 80° (in our measurements the Doppler angle was always much higher), the approximation induces an error in the calculation of V of approximately 1%.

The previously presented bidirectional system has been extended by an additional scanning laser ophthalmoscope (SLO) detection arm measuring the back-reflected intensity for obtaining an en face fundus image. This enables for both selecting the region of interest and gaining information on the orientation of the examined vessels with respect to the detection plane, that is, angle β. The angle β is determined by manually placing the tangent to the vessel at the corresponding position in the captured SLO image (Fig. 1) and calculating the slope with simultaneous consideration of the true dimensions of the SLO image in x and y direction—that is, $w_{sl,x}$ and $w_{sl,y}$, respectively—given by the retinal area scanned by the probing beam, that is, $\beta = \tan^{-1}(w_{sl,x}/w_{sl,y})$. Furthermore, the system includes an additional custom-built fundus view coupled into the OCT sample arm by means of a dichroic mirror. This allows, firstly, for precise focal overlap of the two probe beams onto the region of interest, and, secondly, for inspection of the fundus during measurement.

The bidirectional Doppler OCT system operates at a central wavelength λ of 839 nm. The bandwidth $\Delta\lambda$ of the light source is 52 nm, resulting in an axial resolution in air of 6 μm. The transversal resolution, given by the diameter of the collimated probe beam and the focal length of the focusing lens, is approximately 27 μm for in vitro and 21 μm for in vivo measurements. The oversampling factor (OF) of the phase tomograms is defined as $OF = w \cdot N/d$, where w is the spot size, N is the number of sampling points, and d is the geometric width of the tomogram.[31] With the above given spot size, $N = 2000$ sampling points for both in vitro and in vivo measurements, and a scan width of 1 mm in vitro and 2 mm in vivo, one obtains OFs of 54 and 21, respectively. The power of both probe beams incident on the cornea was measured with 650 μW, which is below the limits of the American National Standard Institute for small-source ocular exposure to a laser beam within the measuring time.[32] The time period between two subsequent CCD recordings (A-scan) was 56 μs, which—with a lateral tomogram dimension of 2000 A-lines for in vivo measurements—gives a frame rate of 9 s^{-1}. The theoretic maximum measurable velocity V_{max} in vivo obtained from equation (1) is approximately 74 mm/s with $\Delta\Phi = 2\pi$, $\beta = 0$, and assuming that the probe beams impinge with their axis of symmetry perpendicularly to the velocity vector. However, since the measurements presented here were performed on vessels around the optic nerve head (ONH), with a distance of approximately one to two disk diameters from its rim, the incidence angle is smaller. Thus, V_{max} without any wrapping artifacts is in the range from 10 to 20 mm/s. Yet, higher velocities can be measured by compensating for these artifacts as described in the next section. The minimum velocity is given by the phase noise $\Delta\Phi_{err}$ present in the system and for a single-beam Doppler OCT system is calculated as $V_{min} = \lambda \cdot \Delta\Phi/(4\pi \cdot \tau)$.[33] This equation, however, only holds true for a Doppler angle of zero degrees that does not occur when measurements are performed in the posterior pole of the eye. With a phase noise $\Delta\Phi_{err} = 0.38$ rad, measured when scanning was performed, the authors were able to assess velocities as low as 1 mm/s.

Doppler Image Acquisition and Processing

For measurements in healthy volunteers, pupils were dilated with one drop of tropicamide (5 mg/mL, MydriaticumAgepha eyedrops; AGEPHA GmbH, Vienna, Austria). Thereafter, the subjects were seated in front of the OCT system and asked to look at the internal fixation target. During measurements the head was stabilized by an adapted slit lamp headrest.

Even though the acquisition of a single tomogram in vivo takes only approximately a tenth of a second, the highly phase-sensitive detection scheme in Doppler OCT still picks up phase offsets due to movements of the subject (Fig. 2A). Therefore, before segmentation of vessels and calculation of blood flow, the phase images were corrected for these background motions. For this purpose, the histogram-based approaches presented by Makita et al.[34] and Schmoll et al.[33] were optimized for movement correction in presence of large vessels. Makita et al.[34] used the change in the position of the maximum of the histogram over time and subtracted the offset from the corresponding A-scans. Schmoll et al.[33] refined this technique by using a third-order polynomial fit to calculate the time course of the maximum position in the histogram.

The modified algorithm used for our measurements takes into account the fact that histograms of A-scans containing vessels not only show a large deviation in the position and magnitude of the maximum, but also are more bumpy because they contain phase information of

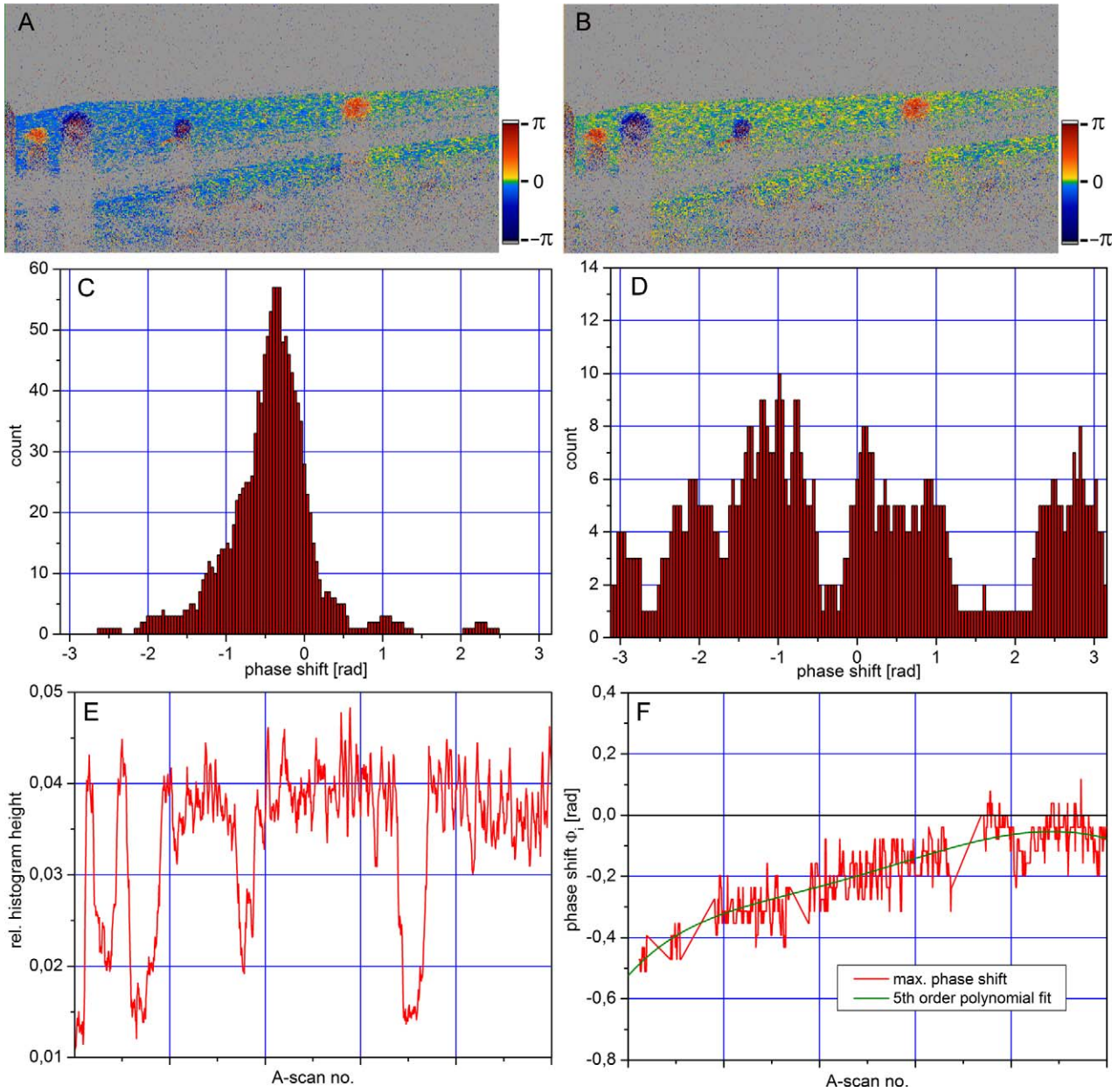

Figure 2. Bulk motion correction. (**A**) Phase tomogram at 20 kHz with bulk motion artifacts. (**B**) Tomogram after modified motion correction algorithm. (**C**) Histogram of a tomogram section containing only tissue. (**D**) Histogram of a tomogram section containing a vessel. (**E**) Histogram maximal height versus A-scan no. Troughs indicate vessel positions. (**F**) Polynomial fit for background motion correction.

both tissue structures and vessels with high blood velocities (Fig. 2D). Thus, the ratio between the maximum value in the histogram and the total number of data points included can be used to distinguish between A-scans containing tissue only and the ones containing vessels. By plotting the above ratio in B-scan direction (Fig. 2E), a threshold for the ratio can be defined to detect the position of the vessels. After identifying the vessels, they are removed from the phase shift curve and the resulting empty positions in the plot are filled by linear interpolation. The resulting phase shift course is then fitted by using a higher-order polynomial fit that accounts more accurately for bulk motion (Fig. 2F). The results presented in this study were gained with a polynomial of order five.

After background motion correction, the vessel position in a preselected region of the phase image was detected by convolution of the image with an elliptic template. The size of the template is manually set to the pixel dimensions of the respective vessel in the tomogram. The values for the phase shift of each channel Φ'_i are in the range $[-\pi, \pi]$. However, especially in arteries and large veins, the flow values can exceed the unambiguous velocity range, which leads to phase-wrapping artifacts, that is, a reversal of the flow direction in the vessel center (Fig. 3A). Such single-phase wraps can easily be corrected by determining the "true" flow direction close to the vessel walls. If the flow inside the vessel has a positive sign, that is, $0 < \Phi' \leq \pi$, and a wrapping artifact in the vessel center occurs, the phases in the center of the vessel are mapped into the range $[0, 2\pi]$ by $\Phi = \Phi' + 2\pi$. On the other hand, if $-\pi \leq \Phi' < 0$, phase-wrapping artifacts are corrected by $\Phi = \Phi' - 2\pi$, and thus, phase shifts Φ are mapped into the range $[-2\pi, 0]$ (Fig. 3B). Double-phase wraps did not occur in any of the veins of the data set.

Owing to the fringe washout—an artifact that occurs in spectrometer-based Doppler OCT when interference fringes move across the CCD pixels during a single exposure—the signal of the moving

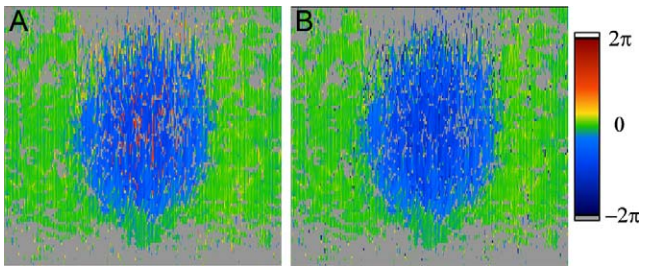

Figure 3. Correction for phase-wrapping artifacts. (**A**) Phase tomogram with wrapping artifacts in positive phase shift direction in the vessel center. (**B**) Phase tomogram after unwrapping by $\Phi = \Phi' - 2\pi$.

structures can get lost. This effect is directly linked to the readout rate of the detector and occurs particularly in the vessel center where the flow velocity of the erythrocytes is highest and in large vessels in close proximity to the ONH. For vessels larger than 90 μm and sufficiently away from bifurcations and junctions, the authors assumed a parabolic flow profile. Therefore, the missing Doppler data are reconstructed by applying a parabolic fit to the available data points.[35] It has previously been shown that the blood velocity profile differs from a parabolic one.[36] However, since only missing data points are reconstructed, while the original data stay untouched, the error introduced by this assumption is expected to be small. This approach gives stable results with respect to the precise reconstruction of the phase information in the central vessel area, as long as the amount of sampling points serving as nodes is sufficient, which was the case in all our measurements.

The independence of lateral and depth dimension of an OCT image—the depth is given by the optical setup of the spectrometer, while the lateral dimension is determined by the scanning range—allows for resampling of the vessel data using bicubic interpolation for achieving equal lateral and axial resolution. This is done under the assumption of a circular vessel cross section and under consideration of the plane at which the probe beam is crossing the vessel (B-scan direction). For calculation of the average phase within the vessel cross section area, the circular approach introduced by Szkulmowska et al.[37] is used. Briefly, the method takes into account the fact that the phase differences Φ' are randomly distributed around the actual values. When phase averaging is performed in the angular domain, this leads to an underestimation of the mean phase difference, especially at high velocities close to the $\pm\pi$ limit. Therefore, the phase values are transformed to complex representation and the averaging is performed by calculating the argument of the complex sum. The average phase shift $\bar{\Phi}_{1,2}$ within a certain vessel is calculated for each frame of a series of 100 to 200 tomograms and for each detection channel separately. Afterwards, the actual phase difference $\Delta\Phi$ between the two probing channels is calculated by the simple subtraction $\Delta\Phi = \Phi_1 - \Phi_2$. For calculation of separation angle $\Delta\alpha$ between the probe beams at the ocular fundus, the parameters of the Gullstrand eye model with a standard eye length of 24.2 mm were assumed.[29] Together with angle β, which is determined from the SLO image, the instantaneous mean absolute flow velocity V_{inst} in the respective vessel was calculated and plotted versus time. Finally, the average flow velocity V_{avg} was computed for 4 to 5 pulse periods.

In Vitro Capillary Measurements

To test the validity of flow velocity estimation with the dual-beam approach, a flow phantom was built. It consisted of a glass capillary with an inner diameter of 300 μm placed in the focal plane of a singlet lens with a focal length of 30 mm. The flow of diluted milk controlled by two different infusion pumps (Precidor Type 5003; INFORS-AG, Basel, Switzerland) and MGVG-Combimat 2000 (MGVG; Doering, Düsseldorf, Germany) was examined with the dual-beam Doppler FD-OCT device. With the pumps, a wide range of velocities could be preselected. The flow velocity was actually measured at 30 different preset velocities ranging from 0.9 to 39.1 mm/s and correlation between preset and measured velocity was examined. This was done five times at each velocity, and mean and standard deviation of these measurements were calculated. For each measurement cycle the feed motion was newly set and measurements were taken with the bidirectional Doppler OCT. The Precidor pump is independent of load and fluctuations in supply voltage, thus providing constant and continuous feed motion. The MGVG Combinat pump is load-dependent and provides higher precision at medium and high velocities.

In Vivo Measurements on Venous Junctions

The study protocol was approved by the Ethics Committee of the Medical University of Vienna. A total of 10 healthy subjects aged between 19 and 35 years participated in this study. The nature of the study was explained to all subjects and they gave written consent to participate. The protocol of the study complied with the standards of the Declaration of Helsinki. An ophthalmic examination, including slit lamp biomicroscopy and indirect funduscopy, was performed. Inclusion criteria were normal ophthalmic findings, ametropia of less than 3 diopters (D), and anisometropia of less than 1 D.

To test the accuracy of the blood flow velocity measurement and blood flow calculation, the total flow in 10 retinal venous junctions of the 10 healthy human volunteers was measured in the two vessels before the junction (daughter vessels 2 and 3) and in the vessel after the junction (source vessel 1). All measurements were done in the temporal retina. Seven bifurcations were located inferiorly and three bifurcations superiorly. In all these experiments retinal vessel diameters were measured in mydriasis with the Dynamic Vessel Analyzer (DVA; IMEDOS GmbH, Jena, Germany). This system comprises a fundus camera (FF 450; Carl Zeiss Meditec AG, Jena, Germany), a high-resolution digital video camera, and a personal computer with analyzing software. For the determination of retinal vessel diameters, recorded images are digitized and analyzed in real-time with a frequency of 50 Hz. The system provides excellent reproducibility and sensitivity.[38,39] After selection of the measurement location, the DVA is able to follow the vessels during movements within the measurement window.

According to the law of mass conservation, the flow through the source vessel needs to equal the sum of the flows in the daughter vessels, that is, $Q_1 = Q_2 + Q_3$. Blood flow in the assessed retinal vessels was calculated as $Q_i = V_{mean,i} \cdot D_i^2\pi/4$ (V_i = velocity in vessel i as assessed by Doppler OCT, D_i = vessel diameter in vessel i as measured with the DVA). In a first step, diameter measurements were performed by using the DVA. The fundus image obtained with this system was used to guide the Doppler OCT measurements. The time interval between the velocity measurements at the three vessels was in the range of 2 to 3 minutes. To assess validity and reproducibility of data, two bifurcations in two subjects were measured five times at different measurement sessions on 5 different study days.

In three subjects, same bifurcations as assessed with Doppler OCT were also measured with a commercially available bidirectional LDV system (LDV-5000; Oculix Inc., Arbaz, Switzerland).[40] The principle of LDV is based on the optical Doppler effect. Laser light of a single-mode laser diode with a wavelength of 670 nm is scattered and reflected by moving erythrocytes, leading to a broadened and shifted homodyne frequency spectrum. The frequency shift is proportional to the blood flow velocity in the retinal vessel. The maximum Doppler shift corresponds to the centerline erythrocyte velocity. The Doppler shift power spectra (DSPS) are recorded simultaneously for two directions of the scattered light. The scattered light is detected in the image plane of the fundus camera. The scattering plane can be rotated and adjusted in alignment with the direction of the velocity vector, which enables absolute velocity measurements. The absolute maximum blood flow velocity is given by $V_{max} = (\lambda \cdot \Delta f)/(n\Delta\ \alpha \cos \beta)$, where λ is again the central wavelength of the incident laser beam and $\Delta f = f_{1max} - f_{2max}$ is

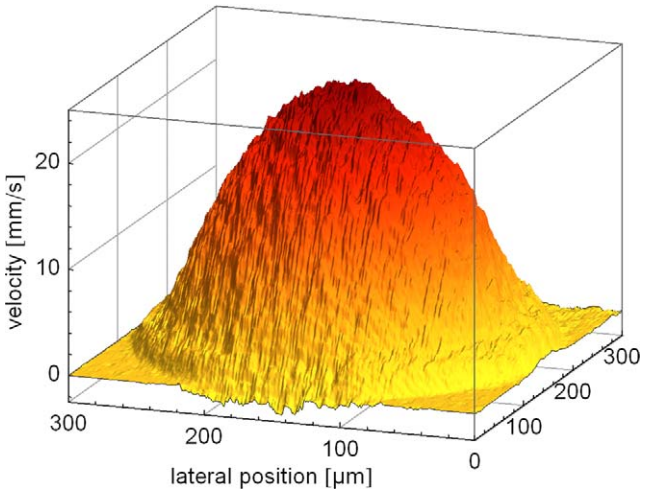

Figure 4. Velocity profile as obtained from a glass capillary perfused with diluted milk.

the difference between the cutoff frequencies, that is, the maximum Doppler shift in the DSPS. n is the refractive index of the flowing medium, $\Delta\alpha$ is the angle between the two wave vectors in which the Doppler signal is detected—congruent with the two probe beams in the bidirectional Doppler OCT system—and β is again the angle between the velocity vector and the detection plane.[40] For comparison of data obtained with both LDV and OCT setups, the mean LDV blood flow velocity within the vessel cross section was calculated as $V_{mean} = V_{max}/2$. Blood flow values as well as velocity values were compared among LDV and Doppler OCT measurements.

Statistical Analysis

Descriptive analysis was used to characterize data. Linear correlation analysis was used to compare the preset values at the pumps and the actually measured values using Doppler OCT. A Bland-Altman plot was used to compare data in source and daughter vessels. In addition, a *t*-test for paired data was used for comparing these data. Reproducibility was assessed by calculating the coefficient of variation. Linear correlation analysis was also performed to characterize the relation between vessel diameters and both blood velocities and blood flow. All data are presented as mean ± SD. A P value <0.05 was considered the level of significance. Statistical analysis was carried out with CSS Statistica for Windows (version 6.0; Statsoft Inc., Tulsa, CA).

Results

In Vitro

Figure 4 shows a velocity profile as obtained with the bidirectional Doppler FD-OCT from diluted milk flowing through a glass capillary. Figure 5 presents the association between measured and preset velocities with the two pumps. A high degree of association was found for both the Precidor Type 5003 ($r = 0.994$, $P < 0.001$) and the MGVG-Combimat 2000 pump ($r = 0.998$, $P < 0.001$), as shown in the left and right panels of Figure 5, respectively.

In Vivo

A total of 10 healthy subjects were examined in the present study. To quantify the uncertainty of our manual segmentation of the angle β, five independent experts segmented β in all 30 vessels included in this study. The mean standard deviation over all vessels was found to be 2°. A typical bifurcation as measured in our experiments is shown in Figure 6. The extracted velocity data from these measurement sites are shown in Figure 7. It is obvious that velocity in all measured vessels showed a high degree of heartbeat synchronous pulsatility. An overview of the obtained results is presented in Table 1. Generally, good agreement was found between the values of blood flow as obtained from the source vessel (Q_1) and the sum of the blood flow values as obtained from the daughter vessels ($Q_2 + Q_3$). This is also evident from the Bland-Altman plot presented in Figure 8. No significant difference was found between Q_1 (11.3 ± 5.2 µL/min) and $Q_2 + Q_3$ (10.7 ± 4.8 µL/min, $P = 0.07$). Table 2 shows the data obtained in two subjects on 5 consecutive days. In both bifurcations, the law of mass conservation was well fulfilled and in all six vessels data were highly reproducible with coefficients of variation between 7% and 16%. Again, good agreement was found on all study days between the values as obtained from the source vessel (Q_1) and the sum of the blood flow values as obtained from the daughter vessels ($Q_2 + Q_3$). No association was found between blood flow values and blood pressure values as expected for an autoregulated vascular bed.

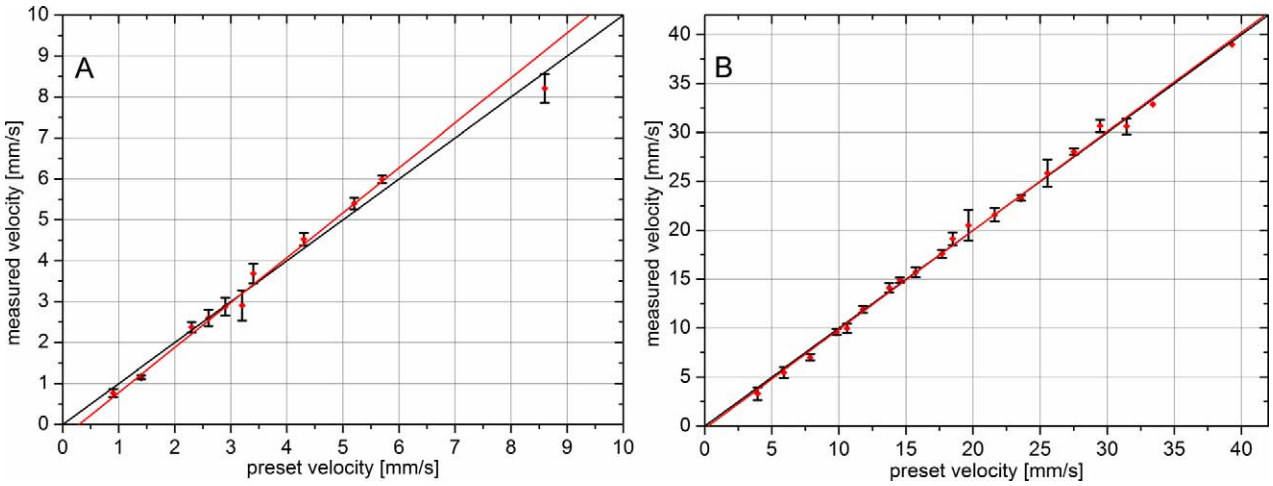

Figure 5. Association between preset and measured flow velocities from a glass capillary perfused with diluted milk for two different pumps: (**A**) Precidor and (**B**) MGVG. *Black line*: unity slope indicating perfect correlation. *Red line*: actual regression line.

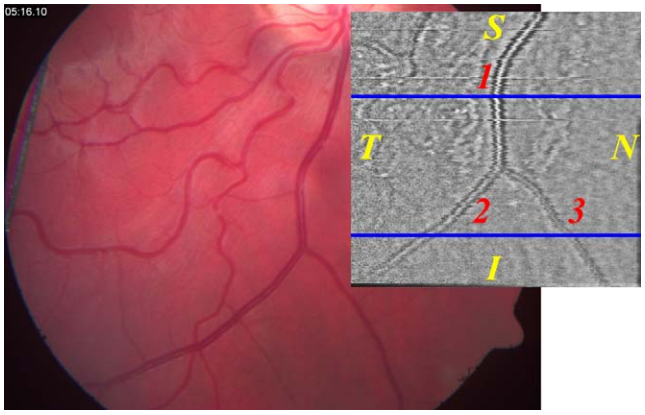

Figure 6. Fundus image and OCT en face image of a bifurcation measured with bidirectional Doppler OCT. The *blue lines* indicate the measurement location.

Figure 9 presents the association between velocities measured with bidirectional Doppler FD-OCT and the vessel diameters as obtained with the DVA. As expected, larger vessel diameters were significantly associated with higher blood velocities ($r = 0.72$, $P < 0.001$). For the relation between blood flow and vessel diameter, linear regression analysis gave a slope of 3.01 ± 0.18 ($r = 0.95$, $P < 0.0001$) (Fig. 10). Table 3 presents the comparison between data as obtained with bidirectional Doppler FD-OCT and the commercially available LDV system in a subgroup of three subjects. Again, agreement was good between measurements, although velocity values, particularly in subject 2, were lower when measured with LDV. Owing to the small number of subjects, no formal statistical analysis was done on these data.

Discussion

Measurement of retinal blood flow is difficult and no method to quantitatively assess perfusion is currently used clinically. This is in part related to the problems of assessing retinal blood flow in vivo. Before any application, a new method has to be carefully evaluated in terms of validity and reproducibility. This is difficult in the absence of a gold standard method. In a previous article,[27] we have shown that bidirectional Doppler OCT allows for precise measurement of velocity of a rotating disk independently of the angle of the disk with respect to the probe beam. This does, however, not sufficiently resemble the in vivo situation. As such, we have added two types of experiments to gain further insight into the validity of the method. Firstly, we have measured velocities of diluted milk pumped through a glass capillary. Excellent agreement between preset and measured velocities was found over a wide range of velocities. Only at higher velocities obtained with the Precidor pump did the measured data show some deviation from the preset values. This is, however, more likely to arise from problems with the pump at high-feed motion than from OCT velocity data extraction.

Secondly, experiments to validate the velocity measurements obtained with bidirectional Doppler OCT were done in vivo. Following the law of mass conservation, the flow value obtained in the source vessel needs to equal the sum of flows in the daughter vessels. This was well fulfilled in all vessel branches studied, with maximum deviations of 15%. With these data, the fact that the studied vessels had wide variation in diameter and flow velocities, as well as β angles, needs to be considered. In addition, the data clearly showed that velocity in the vessels studied is considerably pulsatile (Fig. 7). Thus, reliable data cannot be gained by simply measuring velocities at short intervals; rather, averaging over several pulse periods is required. In arteries, blood flow is even more pulsatile. Owing to the relatively high flow velocities and the limited readout rate of the CCD camera used, arteries were not measured in the present experiments. However, this limitation can easily be overcome by the use of newer generation CCD cameras with higher readout frequencies. We also found good agreement between laser Doppler velocimetry measurements and the data obtained with bidirectional Doppler OCT. In one subject the deviation between measurements was as high as 30%. The reason may be related to problems with the laser Doppler velocimetry measurements rather than the bidirectional Doppler OCT, because the law of mass conservation was better fulfilled when OCT data were taken. A potential problem with LDV is the fact that the laser beam has to hit the center of the vessel to obtain V_{max}. During LDV measurements with the current system, there is no real control to ensure that this is the case except for inspecting the laser beam subjectively through the fundus camera. Owing to slight eye movements, if the laser beam no longer hits the center of the vessel, but only hits the regions of lower flow velocity close to the vessel wall, the system will underestimate V_{max}. On the contrary, Doppler OCT provides velocity information over the whole vessel cross section with the phase tomogram, and thus is less influenced by fixation problems of the subject. To overcome the problem of eye movements during LDV measurements, the Canon apparatus (CLBF100; Canon, Tokyo, Japan) uses an eye-tracking system.[41] The validity measurements of bidirectional Doppler OCT performed in two subjects for 5 days indicate little variability. The variation of flow values in single vessels can be attributed to physiologic fluctuations

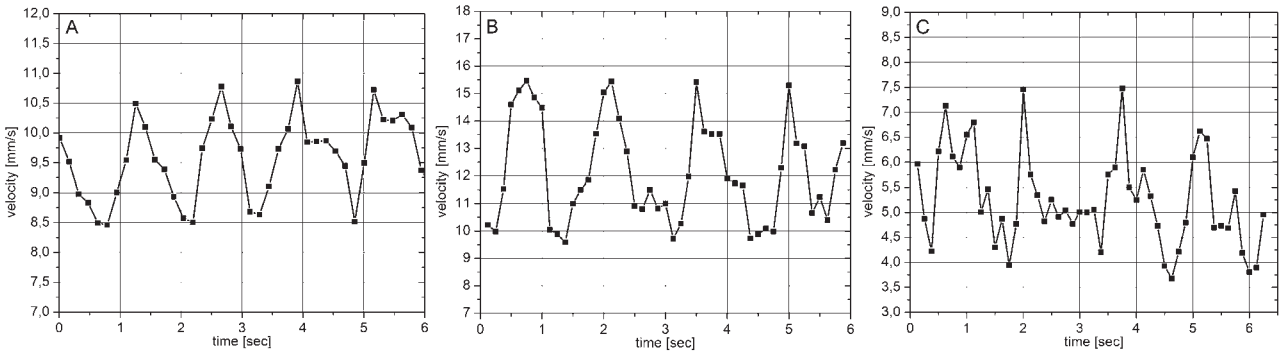

Figure 7. Time courses of blood flow velocity of a single measurement with bidirectional Doppler OCT at the fundus locations shown in Figure 6. (**A**) Position 1. (**B**) Position 2. (**C**) Position 3.

Table 1. Measurements at Retinal Venous Bifurcations in 10 Healthy Subjects

Subject	Vessel	D (μm)	BP_{DVA} (mm Hg)	β (°)	$\Delta\Phi$ (rad)	BP_{OCT} (mm Hg)	V_{avg} (mm/s)	Q (μL/min)
1	1	111	129/72	13	0.85	127/73	8.7	5
1	2	84		1	0.64		6.4	2.1
1	3	98		20	0.72		7.6	3.5
2	1	144	105/67	2	0.76	106/66	7.6	7.4
2	2	105		20	0.63		6.7	3.5
2	3	95		28	0.61		6.9	2.9
3	1	168	111/69	19	0.76	113/71	9.8	13.1
3	2	153		47	0.44		7.9	8.7
3	3	107		5	0.57		7.0	3.8
4	1	172	101/62	15	1.06	99/60	13.4	18.7
4	2	149		45	0.63		10.9	11.4
4	3	130		18	0.45		5.8	4.6
5	1	120	105/67	28	0.51	109/69	7.1	4.8
5	2	94		2	0.38		4.6	1.9
5	3	96		36	0.42		6.3	2.8
6	1	171	120/81	29	0.95	118/79	13.3	18.3
6	2	122		24	0.71		9.5	6.7
6	3	138		18	0.99		12.7	11.4
7	1	150	125/83	22	0.9	123/85	11.8	12.6
7	2	119		42	0.62		10.2	6.8
7	3	105		25	0.76		10.5	5.5
8	1	128	122/76	24	0.6	124/74	8.0	6.2
8	2	94		43	0.35		5.8	2.4
8	3	107		0	0.51		6.2	3.4
9	1	162	109/63	31	0.81	104/64	11.5	14.3
9	2	144		52	0.51		10.1	9.9
9	3	124		2	0.47		5.7	4.2
10	1	166	121/72	1	0.96	122/77	9.6	12.4
10	2	129		60	0.61		12.2	9.5
10	3	92		31	0.45		5.2	2.1

The first vessel in each subject represents the trunk vessel; vessels 2 and 3, the daughter vessels. BP_{OCT}, blood pressure during OCT measurements; BP_{DVA}, blood pressure during DVA measurements; D, vessel diameter; Q, blood flow; DVA, Dynamic Vessel Analyzer; V_{avg}, average velocity within the vessel; β, angle between the orientation of the examined vessels with respect to the detection plane; $\Delta\Phi$, phase difference.

rather than to inaccuracies in the method itself. Further studies in a larger study sample must however be done to investigate the issue of reproducibility in more detail.

Validity of our data is also supported by the linear correlation between blood flow and vessel diameter. This is expected from Murray's law,[42] which predicts that flow should vary with D^3 in vascular beds in which an optimum compromise between blood volume and vascular resistance is found. This is in good agreement with previous laser Doppler velocimetry data published almost 40 years ago.[43] Recently, we have reported that the law is well fulfilled in the human retina, from measurements in 64 healthy subjects.[44] We have observed in this previous study that the correlation line between velocity and diameters is steeper in superior than in inferior quadrants. The present sample size is, however, too small to confirm this result.

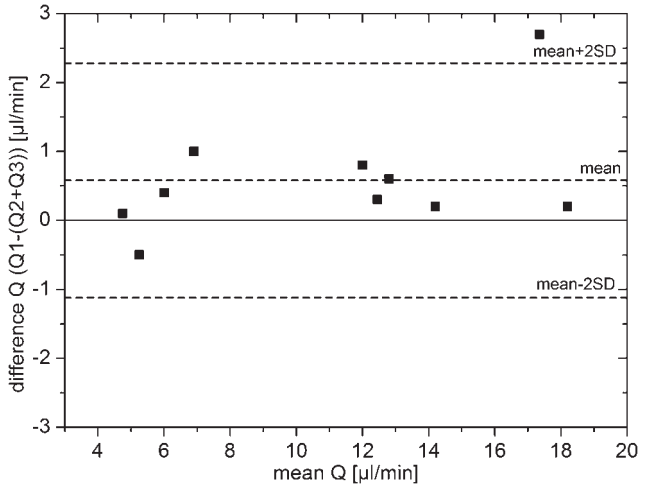

Figure 8. Bland-Altman plot comparing data as obtained between blood flow in the trunk vessel (Q_1) and the sum of blood flow as obtained from the daughter vessels ($Q_2 + Q_3$).

The dual-beam approach has several advantages over conventional single-beam Doppler OCT systems. Firstly, it allows for flow measurements in flat vascular beds, where the incident angle is close to 90° with respect to the velocity vector of interest. If the probe beam impinges perpendicularly to the vessel, there is no velocity vector component in probe beam direction. Hence, in a single-beam Doppler OCT system the measured phase shift amounts to zero. However, if this were the case for one of the probing channels in the bidirectional system, the velocity information of the vessel under study could still be extracted from the other channel. Secondly, measuring with two illumination and detection directions offers a higher precision than the single-beam approach when the angles between velocity and probe beam vector are large. When illuminated with only one probe beam, the erythrocyte velocity V is given by $V = \Phi\lambda/(4\pi \cdot n \cdot \cos\gamma)$, where Φ is the phase shift between subsequent A-line recordings and γ is the angle between probe beam and velocity vector, that is, the Doppler angle. As can be easily

Table 2. Measurements at a Retinal Venous Bifurcation Performed on 5 Consecutive Days in Subjects 6 and 10

Subject	Vessel	D (μm)	Angle β (°)	ΔΦ (rad)	V_{avg} (mm/s)	Q (μL/min)	BP (mm Hg)
6	1	162.7	23	−0.91	10.71	13.36	105/75
6	2	120	27	−0.53	8.27	5.61	
6	3	114.5	10	−0.56	10.26	6.34	
6	1	173	23	−0.79	10.33	14.56	103/71
6	2	111.5	27	−0.45	8.13	4.77	
6	3	139	10	−0.49	9.53	8.68	
6	1	168.3	23	−0.97	10.97	14.64	93/68
6	2	115	27	−0.43	8.00	4.99	
6	3	134	10	−0.71	9.53	8.07	
6	1	175.6	23	−0.91	10.84	15.76	94/64
6	2	122	27	−0.49	8.67	6.08	
6	3	132.5	10	0.42	9.53	7.89	
6	1	169	23	−0.93	12.00	16.16	90/70
6	2	115.2	27	−0.57	7.60	4.75	
6	3	137.8	10	−0.91	10.98	9.82	
10	1	169.3	0	0.91	10.81	14.60	131/82
10	2	135.2	60	0.64	15.21	13.10	
10	3	89.2	31	0.47	6.52	2.44	
10	1	169.2	0	1.05	12.48	16.83	121/75
10	2	133.7	60	0.6	14.26	12.01	
10	3	87.6	31	0.52	7.21	2.61	
10	1	171.4	0	1.03	12.24	16.94	126/74
10	2	140	60	0.63	14.97	13.83	
10	3	94.4	31	0.6	8.32	3.49	
10	1	164.6	0	0.98	11.64	14.87	130/81
10	2	130.9	60	0.74	17.59	14.20	
10	3	85.2	31	0.54	7.49	2.56	
10	1	173.9	0	1.07	12.71	18.12	125/75
10	2	138.4	60	0.72	17.11	15.44	
10	3	94.1	31	0.48	6.65	2.78	

The first vessel represents the trunk vessel; vessels 2 and 3, the daughter vessels. BP, blood pressure.

seen, even small absolute errors in determining the Doppler angle will lead to large variations in calculated velocity owing to the 1/cos γ term. Assuming a true Doppler angle of 86°, an overestimation by only 1° would lead to a value of 0.52 instead of 0.7 in the denominator of the velocity equation, and, thus, to an overestimation of the velocity by almost 50%. If the Doppler angle is very close to 90°, the problem gets even more severe, and very small changes in angle can even lead to changes in the algebraic sign of the phase. Therefore, in single-beam approaches, those data have to be rejected to prevent excessive amplification of the angle error.[35,45] This is also important with slight eye movements when the angle of incidence changes. In such a case, the velocity values yielded from single-beam Doppler OCT will be affected by the eye movements, whereas in the bidirectional detection scheme,

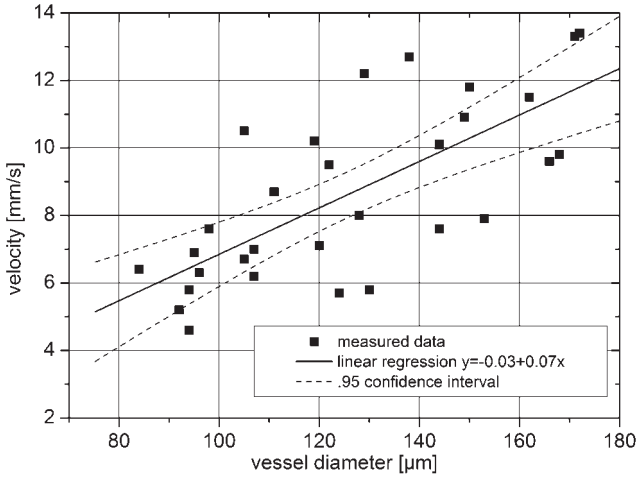

Figure 9. Linear correlation analysis between mean blood velocities as measured with bidirectional Doppler OCT and vessel diameters as measured with the DVA. *Solid line*: best fit result of linear regression (R = 0.95). *Dotted lines*: 95% confidence interval.

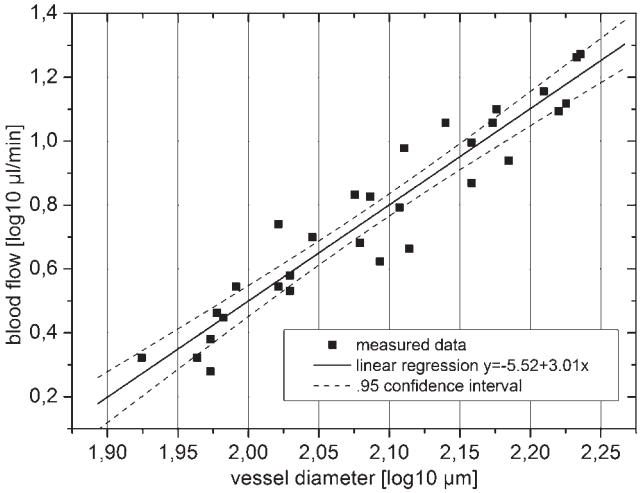

Figure 10. Blood flow versus blood vessel diameter in a log-log scale. *Solid line*: best fit result of linear regression (R = 0.72). *Dotted lines*: 95% confidence interval.

Table 3. Measurements in Three Healthy Subjects at Retinal Venous Bifurcations

Subject	Vessel	D (μm)	BP_{DVA} (mm Hg)	$V_{max,LDV}$ (mm/s)	BP_{LDV} (mm Hg)	$V_{avg,LDV}$ (mm/s)	V_{avg} (mm/s)	BP_{OCT} (mm Hg)
2	1	144	105/67	13.7	102/63	6.9	7.6	106/66
2	2	105		11.3		5.7	6.7	
2	3	95		10.8		5.4	6.9	
9	1	162	109/63	22.6	107/65	11.3	11.5	104/64
9	2	144		17.6		8.8	10.1	
9	3	124		9.2		4.6	5.7	
10	1	166	121/72	16.4	124/75	8.2	9.6	122/77
10	2	129		20.4		10.2	12.2	
10	3	92		10.9		5.5	5.2	

The first vessel represents the trunk vessel; vessels 2 and 3, the daughter vessels. Measurements were done with LDV and bidirectional Doppler OCT. BP_{LDV}, blood pressure during LDV measurements; $V_{avg,LDV}$, average centerline velocity as calculated from LDV data; $V_{max,LDV}$, maximum centerline velocity as measured with LDV.

the observed velocities will remain uninfluenced owing to independence from the Doppler angle, as long as the vessel still lies within the scanned area. One might argue that the $1/\cos\beta$ term in equation (1) is no less of a problem than the critical Doppler angle estimation for the single-beam approach. However, with a standard error of 2° for estimation of β, this leads—for the largest angle ($\beta = 60°$) included in this study—to a deviation of only 6.5% in flow velocity. Another issue that is critical is that both beams have to be focused at the same location, that is, their foci have to overlap. This can, however, easily be achieved by means of the fundus view. The quality of the measurement can be judged by looking at the phase shift courses of the two channels that have to run in parallel.

Besides the fact that precision of bidirectional LDV is strongly dependent on exact focusing of the probe beam onto the vessel center, it only permits measurement of a single vessel. Thus, assessment of total retinal flow, that is, measurement of all major arteries and veins leaving and entering the ONH, requires a relatively long acquisition time of approximately 20 minutes (Garhöfer G, Schmetterer L, Werkmeister RM, et al., unpublished observations, 2012). In contrast, by simply increasing the scanning range, OCT offers information about blood flow velocities in several neighboring vessels; thus, using a squared detection scheme around the ONH would decrease the measurement time to approximately four times 1 minute, including the time needed for alignment of the subject, search of the region of interest, and overlap of the focal planes of the probe beams. Other problems with LDV include the calculation of the maximum Doppler frequency shift from the power spectrum corresponding to the maximum center velocity within the retinal vessel and the assumption of a parabolic flow profile.

A difference between all previous measurements of retinal blood flow, using OCT technology[33,35,46–49] and the present approach, is the use of a fundus camera–based device to measure retinal vessel diameters. The DVA is a very well-established technique to measure retinal vessel diameters and provides absolute values in emmetropic eyes.[39] Other investigators have used phase tomograms obtained with Doppler OCT to extract diameter data. The precision of this extraction is of course limited by the axial resolution of the OCT system used, which is typically between 4 and 6 μm depending on the light source used. In addition, one needs to consider that the determination of the diameters relies on phase shift data and that the lower limits for detection of blood velocities differ for different Doppler OCT systems, depending on the intrinsic phase noise. Hence, very low velocities in close proximity to the vessels walls cannot be measured or rather are covered by the noise. In addition, there is an erythrocyte-free region close to the vessel wall, from which no Doppler data are received, because this region consists of plasma only. Theoretically, this should lead to an underestimation of retinal vessel diameters when extracted from phase tomograms, although an experimental verification of this assumption is lacking.

One needs to consider that, in the present study, measurements of retinal blood velocities and retinal vessel diameters were not done simultaneously. This represents a shortcoming of our method as compared to other techniques that allow for extraction of both velocity and diameter data from OCT phase images.[31,35,46,47] However, one also needs to take into account that the data presented in our study were collected within a few minutes and that hemodynamic conditions were stable. Moreover, the bidirectional OCT system may in principle be coupled to the Zeiss FF450 fundus camera, and this possibility is currently being investigated in our laboratory.

In conclusion, quantitative measurements of absolute blood flow velocity and absolute volumetric blood flow in retinal vessels of healthy human subjects can be done with high validity by combining velocity extraction using bidirectional Doppler OCT with diameter measurements using the DVA.

References

1. Pemp B, Schmetterer L. Ocular blood flow in diabetes and age-related macular degeneration. *Can J Ophthalmol*. 2008;43:295–301.
2. Mozaffarieh M, Grieshaber MC, Flammer J. Oxygen and blood flow: players in the pathogenesis of glaucoma. *Mol Vis*. 2008;14:224–233.
3. Stalmans I, Vandewalle E, Anderson DR, et al. Use of colour Doppler imaging in ocular blood flow research. *Acta Ophthalmol*. 2011;89:e609–e630.
4. Lieb WE, Cohen SM, Merton DA, Shields JA, Mitchell DG, Goldberg BB. Color Doppler imaging of the eye and orbit: technique and normal vascular anatomy. *Arch Ophthalmol*. 1991;109:527–531.
5. Feke GT, Riva CE. Laser Doppler measurements of blood velocity in human retinal vessels. *J Opt Soc Am*. 1978;68:526–531.
6. Riva CE, Grunwald JE, Sinclair SH, Petrig BL. Blood velocity and volumetric flow rate in human retinal vessels. *Invest Ophthalmol Vis Sci*. 1985;26:1124–1132.
7. Feke GT, Tagawa H, Deupree DM, Goger DG, Sebag J, Weiter JJ. Blood flow in the normal human retina. *Invest Ophthalmol Vis Sci*. 1989;30:58–65.
8. Grunwald JE, Riva CE, Baine J, Brucker AJ. Total retinal volumetric blood flow rate in diabetic patients with poor glycemic control. *Invest Ophthalmol Vis Sci*. 1992;33:356–363.

9. Garcia JP Jr, Garcia PT, Rosen RB. Retinal blood flow in the normal human eye using the canon laser blood flowmeter. *Ophthalmic Res*. 2002;34:295–299.
10. Rechtman E, Harris A, Kumar R, et al. An update on retinal circulation assessment technologies. *Curr Eye Res*. 2003;27: 329–343.
11. Yannuzzi LA, Rohrer KT, Tindel LJ, et al. Fluorescein angiography complication survey. *Ophthalmology*. 1986;93: 611–617.
12. Leila L. Adverse effects of fluorescein angiography. *Acta Ophthalmol Scand*. 2006;84:720–721.
13. Huang D, Swanson EA, Lin CP, et al. Optical coherence tomography. *Science*. 1991;254:1178–1181.
14. Fercher AF, Hitzenberger CK, Drexler W, Kamp G, Sattmann H. In vivo optical coherence tomography. *Am J Ophthalmol*. 1993;116:113–114.
15. Wojtkowski M, Leitgeb R, Kowalczyk A, Bajraszewski T, Fercher AF. In vivo human retinal imaging by Fourier domain optical coherence tomography. *J Biomed Opt*. 2002;7:457–463.
16. Leitgeb R, Drexler W, Unterhuber A, et al. Ultrahigh resolution Fourier domain optical coherence tomography. *Opt Express*. 2004;12:2156–2165.
17. Unterhuber A, Povazay B, Hermann B, Sattmann H, Chavez-Pirson A, Drexler W. In vivo retinal optical coherence tomography at 1040 nm—enhanced penetration into the choroid. *Opt Express*. 2005;13:3252–3258.
18. Makita S, Fabritius T, Yasuno Y. Full-range, high-speed, high-resolution 1 micron spectral-domain optical coherence tomography using BM-scan for volumetric imaging of the human posterior eye. *Opt Express*. 2008;16:8406–8420.
19. Schmidt-Erfurth U, Leitgeb RA, Michels S, et al. Three-dimensional ultrahigh-resolution optical coherence tomography of macular diseases. *Invest Ophthalmol Vis Sci*. 2005;46: 3393–3402.
20. Ahlers C, Gotzinger E, Pircher M, et al. Imaging of the retinal pigment epithelium in age-related macular degeneration using polarization-sensitive optical coherence tomography. *Invest Ophthalmol Vis Sci*. 2010;51:2149–2157.
21. Bolz M, Kriechbaum K, Simader C, et al. In vivo retinal morphology after grid laser treatment in diabetic macular edema. *Ophthalmology*. 2010;117:538–544.
22. Leitgeb R, Schmetterer L, Drexler W, Fercher A, Zawadzki R, Bajraszewski T. Real-time assessment of retinal blood flow with ultrafast acquisition by color Doppler Fourier domain optical coherence tomography. *Opt Express*. 2003;11:3116–3121.
23. White B, Pierce M, Nassif N, et al. In vivo dynamic human retinal blood flow imaging using ultra-high-speed spectral domain optical coherence tomography. *Opt Express*. 2003;11: 3490–3497.
24. Pedersen CJ, Huang D, Shure MA, Rollins AM. Measurement of absolute flow velocity vector using dual-angle, delay-encoded Doppler optical coherence tomography. *Opt Lett*. 2007;32: 506–508.
25. Iftimia NV, Hammer DX, Ferguson RD, Mujat M, Vu D, Ferrante AA. Dual-beam Fourier domain optical Doppler tomography of zebrafish. *Opt Express*. 2008;16:13624–13636.
26. Makita S, Jaillon F, Yamanari M, Miura M, Yasuno Y. Comprehensive in vivo micro-vascular imaging of the human eye by dual-beam-scan Doppler optical coherence angiography. *Opt Express*. 2011;19:1271–1283.
27. Werkmeister RM, Dragostinoff N, Pircher M, et al. Bidirectional Doppler Fourier-domain optical coherence tomography for measurement of absolute flow velocities in human retinal vessels. *Opt Lett*. 2008;33:2967–2969.
28. Tuchin VV. *Optical Clearing of Tissue and Blood*. Bellingham, WA: SPIE Publications; 2005.
29. Gullstrand A. The dioptrics of the eye. In: Southall J, ed. *Helmholtz's Treatise on Physiological Optics*. Washington, DC: Optical Society of America; 1924;351–352.
30. Norrby S, Piers P, Campbell C, van der Mooren M. Model eyes for evaluation of intraocular lenses. *Appl Opt*. 2007;46:6595–6605.
31. Singh AS, Schmoll T, Leitgeb RA. Segmentation of Doppler optical coherence tomography signatures using a support-vector machine. *Biomed Opt Express*. 2011;2:1328–1339.
32. American National Standards Institute. *American National Standard for Safe Use of Lasers*. Orlando, FL: The Laser Institute of America; 2000. ANSI Z136.1-2000.
33. Schmoll T, Kolbitsch C, Leitgeb RA. Ultra-high-speed volumetric tomography of human retinal blood flow. *Opt Express*. 2009;17:4166–4176.
34. Makita S, Hong Y, Yamanari M, Yatagai T, Yasuno Y. Optical coherence angiography. *Opt Express*. 2006;14:7821–7840.
35. Singh AS, Kolbitsch C, Schmoll T, Leitgeb RA. Stable absolute flow estimation with Doppler OCT based on virtual circumpapillary scans. *Biomed Opt Express*. 2010;1:1047–1058.
36. Zhong Z, Song H, Chui TY, Petrig BL, Burns SA. Non-invasive measurements and analysis of blood velocity profiles in human retinal vessels. *Invest Ophthalmol Vis Sci*. 2011;52:4151–4157.
37. Szkulmowska A, Szkulmowski M, Kowalczyk A, Wojtkowski M. Phase-resolved Doppler optical coherence tomography—limitations and improvements. *Opt Lett*. 2008;33:1425–1427.
38. Polak K, Dorner G, Kiss B, et al. Evaluation of the Zeiss retinal vessel analyser. *Br J Ophthalmol*. 2000;84:1285–1290.
39. Garhofer G, Resch H, Sacu S, et al. Effect of regular smoking on flicker induced retinal vasodilatation in healthy subjects. *Microvasc Res*. 2011;82:351–355.
40. Riva CE, Grunwald JE, Sinclair SH, O'Keefe K. Fundus camera based retinal LDV. *Appl Opt*. 1981;20:117–120.
41. Yoshida A, Feke GT, Mori F, et al. Reproducibility and clinical application of a newly developed stabilized retinal laser Doppler instrument. *Am J Ophthalmol*. 2003;135:356–361.
42. Murray CD. The physiological principle of minimum work, I: the vascular system and the cost of blood volume. *Proc Natl Acad Sci U S A*. 1926;12:207–214.
43. Riva C, Ross B, Benedek GB. Laser Doppler measurements of blood flow in capillary tubes and retinal arteries. *Invest Ophthalmol*. 1972;11:936–944.
44. Garhöfer G, Werkmeister RM, Dragostinoff N, Schmetterer L. Retinal blood flow in healthy young subjects. *Invest Ophthalmol Vis Sci*. 2012. In press.
45. Wang Y, Lu A, Gil-Flamer J, Tan O, Izatt JA, Huang D. Measurement of total blood flow in the normal human retina using Doppler Fourier-domain optical coherence tomography. *Br J Ophthalmol*. 2009;93:634–637.
46. Wang Y, Fawzi A, Tan O, Gil-Flamer J, Huang D. Retinal blood flow detection in diabetic patients by Doppler Fourier domain optical coherence tomography. *Opt Express*. 2009;17:4061–4073.
47. Baumann B, Potsaid B, Kraus MF, et al. Total retinal blood flow measurement with ultrahigh speed swept source/Fourier domain OCT. *Biomed Opt Express*. 2011;2:1539–1552.
48. Wang Y, Bower BA, Izatt JA, Tan O, Huang D. Retinal blood flow measurement by circumpapillary Fourier domain Doppler optical coherence tomography. *J Biomed Opt*. 2008;13: 064003.
49. Wang Y, Fawzi AA, Varma R, et al. Pilot study of optical coherence tomography measurement of retinal blood flow in retinal and optic nerve diseases. *Invest Ophthalmol Vis Sci*. 2011;52:840–845.